Multiple ionization of He^+–rare-gas collisions

R. D. DuBois
Pacific Northwest Laboratory, Richland, Washington 99352
(Received 27 June 1988)

Absolute cross sections are presented for single and multiple ionization of He, Ne, Ar, and Kr resulting from He^+ impact between 15 and 2000 keV. The cross sections are measured for collisions in which the projectile charge state is unchanged (direct ionization), decreases (single-electron capture), and increases (single-electron loss). From these data total cross sections for target-ion production, for free-electron production, and for single-electron capture are determined. The data are used to demonstrate the relative importance of the various ionization channels as they contribute to the production of free electrons. In addition, from the electron-loss data, it is deduced that electron loss by the projectile generally results in ionization of the target as well.

INTRODUCTION

Although there have been many experimental studies of multiple ionization of atoms by bare-ion impact, very little information is available for light, partially stripped projectiles. This paper is intended to partially fill that void. Absolute single- and multiple-target-ionization cross sections are presented for He^+ ions colliding with He, Ne, Ar, and Kr atoms. The channels studied include single- and multiple-target ionization resulting from direct ionization (meaning that the projectile charge state does not change as a result of the collision), from single-electron capture by the projectile, and from single-electron loss by the projectile.

The measured cross sections are combined in various fashions to obtain total-positive-ion, free-electron, electron-capture, and electron-loss cross sections, thus providing a detailed picture of ionization occurring as a result of He^+ impact. By comparing the individual and the total cross sections, the relative contribution of the various ionization channels to the production of target ions and free electrons is demonstrated.

Previous experimental studies of ionization of rare gases by energetic He^+ impact include numerous measurements of total ionization and electron transfer cross sections (see Refs. 1–6 and references contained therein). There have also been theoretical attempts at calculating total ionization and electron-transfer cross sections for He^+ impact.[7–9] A few investigations of multiple target ionization have been made, but these generally have concentrated on studies of total multiple ionization probabilities.[10–14] In a few cases, multiple ionization measurements have been reported where the type of collision (e.g., charge transfer or direct ionization) is specified. For example, for low-energy He^+ impact, multiple-target ionization resulting from electron capture has been investigated for He, Ne, Ar, Kr, and Xe targets[15,16] and direct multiple ionization has been studied for all but Xe targets.[16] However, prior to this work, the electron loss channels have not been studied.

Thus, this work is intended to add to our knowledge of multiple ionization of atoms resulting from He^+ impact by extending the measurements to higher impact energies where electron capture by the projectile is becoming relatively less important with respect to direct ionization, but electron loss from the projectile is gaining in importance. Included in the data presented here are previously reported[16] cross sections (15–100 keV) which have been reevaluated to account for new information available[17] regarding detection efficiencies for the recoil target ions. In addition, the previously reported cross sections have been renormalized to the total ion production cross sections of Rudd *et al.*[1] in order to provide consistency with the present higher-energy results. This normalization and reevaluation of detection efficiencies account for the small discrepancies (generally on the order of 10%) between the data presented here with those presented in an earlier publication based on preliminary measurements.[18]

EXPERIMENTAL PROCEDURE

The experimental apparatus and procedure used to measure single- and multiple-ionization cross sections for He^+ impact are identical to that used for He^{2+} impact[17] to which the reader is referred for additional information. Summarized briefly, relative multiple-ionization cross sections were measured by passing a He^+ beam though a gas cell, extracting the resultant target ions with a small electric field, and counting those ions in coincidence with post-collision charge state analyzed projectile ions. Since only one post-collision beam detector was used, sequential measurements for the singly charged, neutral, and doubly charged post-collision components of the beam as well as for the entire post-collision beam were performed. In all cases, data were collected for known target gas pressures and He^+ beam intensities. Hence data for the various channels could be related to each other and relative cross sections for direct ionization, electron capture, and electron loss as well as for total multiple ionization could be obtained. Generally the sum of the cross sections for the individual interaction channels agreed with the total cross section obtained using the entire post-collision beam to within approximately 10%.

The relative cross sections were then placed on an ab-

solute scale by normalizing at each impact energy to the total absolute slow positive charge production cross sections σ_+ or Rudd *et al.*,[1] i.e., $\sigma_+ = \sum_q q\sigma_q^T$. Here σ_q^T is the total cross section for producing a target ion with charge q, i.e., the target charge state distributions obtained for all possible final charge states of the projectile. This total cross section consists of contributions from the direct-ionization ($j=1$), electron-capture ($j=0$), and electron-loss ($j=2$) channels, i.e., $\sigma_q^T = \sum_q \sigma_q^{1j}$, where the superscript 1 designates the incoming projectile charge state. Contributions due to double capture were neglected since they are negligible for the data presented here.[2]

From the individually measured cross sections, it is possible to determine total cross sections for free-electron production, e.g., $\sigma_- = \sum_q (q-1+j)\sigma_q^{1j}$ and for single-electron capture, e.g., $\sigma^{10} = \sum_q \sigma_q^{10}$. In the case of electron loss, the sum of the present cross sections, $\sum_q \sigma_q^{12}$, is smaller than the total electron-loss cross section σ^{12} by an amount equal to the "pure" electron-loss cross section σ_0^{12}, e.g., when only the projectile is ionized. Thus, the individual cross sections reported here can be combined in various fashions to supplement our knowledge about total cross sections and these total cross sections can be used to test the accuracy of the present measurements.

As was done previously for He^{2+} impact,[17] the absolute cross sections presented here are averages of data obtained for several different experimental configurations, e.g., target-ion detector orientation, extraction voltage, and flight-tube design, etc. Generally the reproducibility of the cross sections obtained for these various configurations was $\pm 15\%$; which, when combined with the 10% uncertainties in the absolute σ_+ cross sections used to place the data on an absolute scale, indicates an overall uncertainty of $\pm 18\%$. In certain cases, indicated with asterisks in the cross section tables, the reproducibility was poorer and the overall uncertainty larger (typically 25–30%). In addition, larger absolute uncertainties may exist for the lowest impact energies due to larger uncertainties in the σ_+ cross sections that were used for normalization purposes.

As mentioned above, the cross sections that were reported in Ref. 16 for impact energies less than 100 keV have been renormalized and slightly modified to account for new information available about the target-ion detection efficiencies. Originally these data were normalized to total electron-capture cross sections σ^{10}; but this resulted in a total ion production cross section σ_+ that was approximately 10–15% smaller than the values quoted in Ref. 1. Since normalization to σ^{10} was not always possible at higher impact energies due to unavailability of accurately known electron-capture cross sections, for consistency all the data presented here have been normalized to the σ_+ cross sections reported in Ref. 1.

In spite of this renormalization and detection efficiency corrections, it will be shown that total electron-production cross sections σ_- obtained from the present data deviate from the values quoted in Ref. 1 for impact energies below 100 keV. The same phenomenon was observed for He^{2+} impact on the same targets.[17] In order to investigate this discrepancy, the cross section measurements were recently repeated in the 50–150-keV energy range. These measurements were performed using our 2-MV Van de Graaff accelerator; hence it was not possible to investigate lower impact energies. It should be emphasized, however, that these recent measurements were performed using an entirely different target, target-ion detection system, and projectile-ion detection system than were used to collect the data reported in Ref. 16. The major differences between the newest system and the one described in Ref. 17 are a modification of the target-ion flight tube and detection system to accommodate a Z-configuration channel-plate detector and expansion of the projectile-ion detection system to enable simultaneous detection of the ionization, capture, and loss channels.

The system was independently calibrated to provide absolute cross sections without normalization to total capture or positive ion-production cross sections at each impact energy as was required previously. This calibration primarily required determination of the projectile- and target-ion detection efficiencies. The projectile-ion detection efficiencies were determined for each of the detectors by comparing their counting rates with those measured by a surface barrier detector for which unit efficiency was assumed. The measured efficiencies were found to be independent of projectile-ion charge state and impact energy in the 200–1500-keV range and were assumed to be the same for lower impact energies. The absolute target-ion detection efficiencies were determined in the following manner. First it was demonstrated that the target-ion signal was independent of extraction fields for fields above approximately 20 V/cm (200 V/cm were used for data collection) and were directly proportional to the target gas pressure. Then relative detection efficiency curves were obtained by varying the voltage on the front surface of the detector (a Z-configuration channel plate) while keeping the gain across the detector constant. These relative detection efficiencies were then placed on an absolute scale by normalizing measured coincidence signals to total single ionization cross sections for 1-MeV H^+ impact.[19] This required assuming that all geometric quantities are known but since the cross sections are proportional to the product of the geometrical quantities and the detection efficiencies, any inconsistencies in this assumption are removed. The resultant detection efficiencies measured for the channel-plate detector are nearly identical to those shown in Ref. 17 for target ions directly impinging on a channeltron.

Absolute cross sections measured using this new system have experimental uncertainties of 18–50% depending on the size of the cross section. As will be shown, within experimental uncertainties, the recent data confirm our previous results and there remains an unresolved inconsistency between total electron-production cross sections obtained using the present data with those presented in Ref. 1.

RESULTS AND DISCUSSION

Absolute cross sections for He^+-impact ionization of He, Ne, Ar, and Kr targets are presented in Tables I–IV,

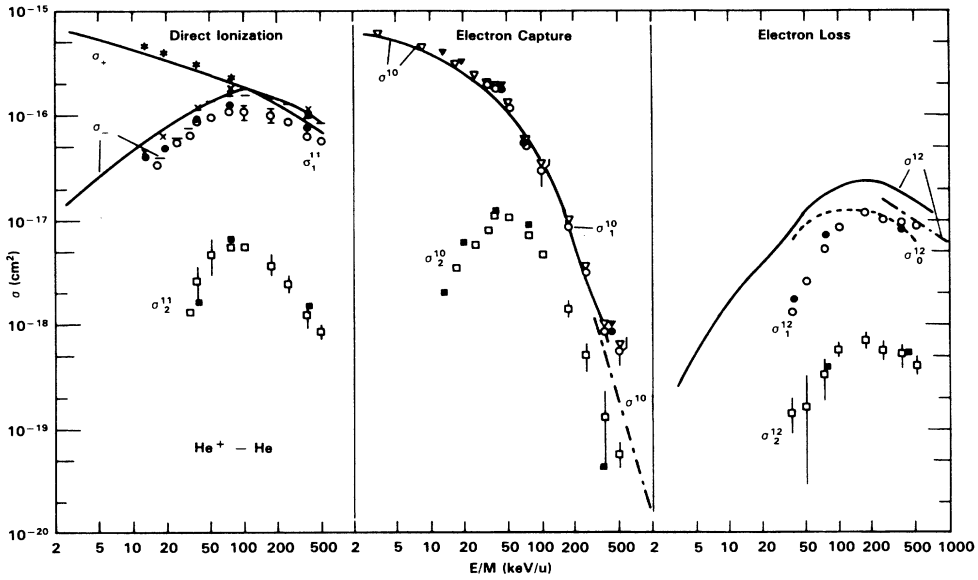

FIG. 1. Absolute cross sections for multiple ionization of helium by He^+ impact. σ^+: ——, total positive-charge production cross sections from Ref. 1 used for normalization; *, remeasurement. σ_-: ——, total free electron production cross section Ref. 1; –, present work; ×, remeasurement. σ^{10}: ——, total single-electron-capture cross sections from Refs. 1–3; —·—·—·, from Ref. 6; ▽, present work. σ^{12}: ——, total single-electron-loss cross sections from Refs. 1 and 2; —·—·—·, from Ref. 6. σ_q^{1j}: cross sections for single (○) and double (□) ionization of helium, $q=1,2$, respectively. The superscripts represent the projectile initial and final charge states. σ_0^{12}: · · · ·, cross sections for "pure" electron loss by the projectile deduced from $\sigma^{12}-\sum_q \sigma_q^{12}$. The error bars represent reproducibility of repeat measurements unless the reproducibility was within the size limits of the symbols used to graph the data. The dashed curves are only to guide the eye. Remeasured values as described in the text are shown with closed symbols.

respectively. These tabulations do not include the recently remeasured cross sections which are primarily intended to verify the earlier measurements. Graphical representations of the data are also included for discussion purposes.

Helium

Cross sections for the individual channels leading to ionization of helium are listed in Table I and shown in Fig. 1. The closed symbols indicate recent data measured

TABLE I. Absolute cross sections (in units of 10^{-16} cm^2) for He^+-He collisions. σ_q^{1j} ($j=1,0,2$) are for direct ionization, single electron capture, and electron loss, respectively; σ_+, total positive ion production cross sections from Ref. 1 used for normalization purposes; σ_-, total free-electron production cross sections obtained from present σ_q^{1j} cross sections as described in the text; σ_0^{12}, cross sections for "pure" electron loss, i.e., no target ionization accompanying the projection ionization, obtained by subtracting $\sum_q \sigma_q^{12}$ from σ^{12}. The 3.75–33.3 keV/u cross sections are taken from Ref. 16 and have been reevaluated as described in the text. Typical uncertainties are ±18% except for those values indicated with asterisks which have 25–30 % uncertainties.

			He^+-He							
			Direct ionization			Electron capture			Electron loss	
E/M (keV/u)	σ_+	σ_-	σ_1^{11}	σ_2^{11}	σ^{10}	σ_1^{10}	σ_2^{10}	σ_0^{12}	σ_1^{12}	σ_2^{12}
3.33	5.9				5.9	5.9				
8.33	4.5				4.5	4.5				
16.7	3.5	0.391	0.339		3.10	3.06	0.0348			
25.0	3.05	0.600	0.542		2.44	2.39	0.0591			
33.3	2.8	0.754	0.647	0.0129	2.05	1.97	0.0817			
37.5	2.7	1.14	0.882	0.0268*	1.91	1.79	0.113	0.066	0.0130	0.001 41*
50	2.4	1.33	0.975	0.0481*	1.30	1.20	0.106	0.097	0.0263	0.001 67*
75	2.0	1.51	1.08	0.0553	0.575	0.503	0.0719	0.127	0.0544	0.003 31*
100	1.8	1.54	1.07	0.0545	0.348*	0.300*	0.0475	0.119	0.0886	0.005 84
175	1.4	1.45	1.00	0.0386*	0.103	0.0886	0.0140	0.105	0.118	0.007 17
250	1.1	1.27	0.879	0.0248*	0.0369*	0.0317	0.005 22*	0.114	0.100	0.005 84*
375	0.83	0.949	0.628	0.0127*	0.0100	0.008 71	0.001 30*	0.081	0.0985	0.005 30*
500	0.68	0.826	0.560	0.0087	0.006 41*	0.005 83*	0.000 584*	0.061	0.0871*	0.004 15*

using the absolutely calibrated system described above while data obtained via normalization to total ion production cross sections are shown with open symbols. The agreement between the two sets of data are within combined experimental uncertainties although the new measurements are consistently 20% larger.

Included in the figure are previously measured total cross sections which can be compared to total cross sections obtained by appropriately summing the present data. The present total electron-production cross sections σ_-, are seen to be in excellent agreement with those reported by Rudd *et al.*[1] for impact energies above 100 keV but as the impact energy is decreased, the present cross sections become progressively smaller. This discrepancy is confirmed by the remeasured cross sections—particularly if one were to normalize the remeasured cross sections to the σ_+ values of Ref. 1. Similar discrepancies for σ_- will be shown to occur for all targets investigated here and was also observed to occur when the same targets are ionized by He^{2+} ions.[17] A discussion of this discrepancy will be given after all of the data are presented.

In the electron-capture channel, the present total capture cross sections are 10–20% larger than those measured previously[1–3,6] except at the highest energies where larger discrepancies are indicated. For impact energies larger than 100 keV/u, capture plus ionization σ_2^{10} is approximately a factor of 5 less probable than is pure electron capture σ_1^{10}.

The data in Fig. 1 also demonstrate that the sum of the electron-loss cross sections $(\sigma_1^{12}+\sigma_2^{12})$ is considerably smaller than the total electron-loss cross sections σ^{12} reported in Refs. 1 and 2 and is somewhat smaller than the σ^{12} cross sections reported in Ref. 6. This difference is attributed to "pure" electron loss σ_0^{12}, which is unobservable in the present experiment since it does not produce a target ion. However, the σ_0^{12} cross section can be deduced by subtracting $\sum_q \sigma_q^{12}$ from the total loss cross section. For this subtraction the σ^{12} cross sections reported in Refs. 1 and 2 were used and the resulting σ_0^{12} cross sections are indicated by the dotted curve in Fig. 1. These data indicated that "pure" electron loss dominates the electron-loss channel at lower impact energies but as the impact energy increases, electron loss by the projectile is likely to result in ionization of the target as well.

Overall, Fig. 1 demonstrates that double target ionization occurring in He^+-He collisions is roughly an order of magnitude less likely than is single ionization. This is true for all impact energies and ionization channels investigated. However, double ionization can still be an important contributor to the total free electron production cross section. For example, at low impact energies, double ionization resulting from electron-capturing collisions accounts for approximately 10% of the free-electron production. This is demonstrated in Fig. 2 where the relative importance of the direct-ionization, electron-capture, and electron-loss channels to the total electron production is shown. At higher energies, approximately 30% of the free-electron production occurs as a result of collisions in which the projectile loses an electron. In this

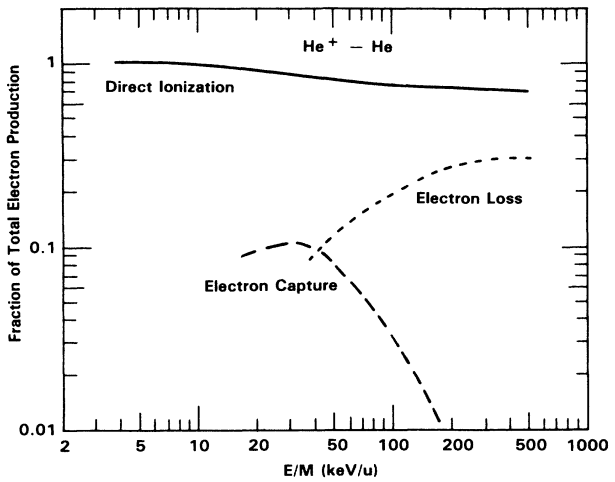

FIG. 2. Fraction of free-electron production due to direct-ionization, electron-capture, and electron-loss channels in He^+-He collisions.

case, according to Fig. 1, approximately half of the time the projectile loses its electron and the target also loses an electron. Thus two electrons are released to the continuum. Approximately 4% of the time, the He^+ ion loses its electron and the helium target loses both electrons—thus releasing three electrons to the continuum.

There are no other data available for testing the accuracy of the individual cross sections shown in Fig. 1. However, the individual cross sections can be used to determine total single- and double-target ionization cross sections, σ_1^T and σ_2^T, which have previously been measured. A comparison of the present and previous results[5,10,11,13] is shown in Fig. 3. Note that the measurements made several years ago in our laboratory[11] have been corrected for target-ion detection efficiencies and then normalized to σ_+ cross sections[1] in order to obtain absolute cross sections that are shown in Fig. 3. For single-target ionization all of the data agree within experimental uncertainties although the values reported by Wood *et al.*[13] are consistently 20% smaller.

At first glance, the situation for double ionization is less clear. Here the present measurements are in better agreement with the early measurements of Fedorenko and Afrosimov[10] at lower energies while the values reported by Wood *et al.*[13] are roughly 40% smaller—nearly agreeing with cross sections obtained from our previous work.[11] However, the single-ionization cross-section data imply that half of this discrepancy can be accounted by the absolute normalization used and thus the double-to-single-ionization ratios of Wood *et al.* differ from the present values by less than 20%. Hence the present work and that of Refs. 10 and 13 are all in reasonable agreement with the double-ionization cross sections obtained from our earlier work being 50–60% smaller. Since the impact-velocity dependencies are the same and similar discrepancies were observed for H^+-He

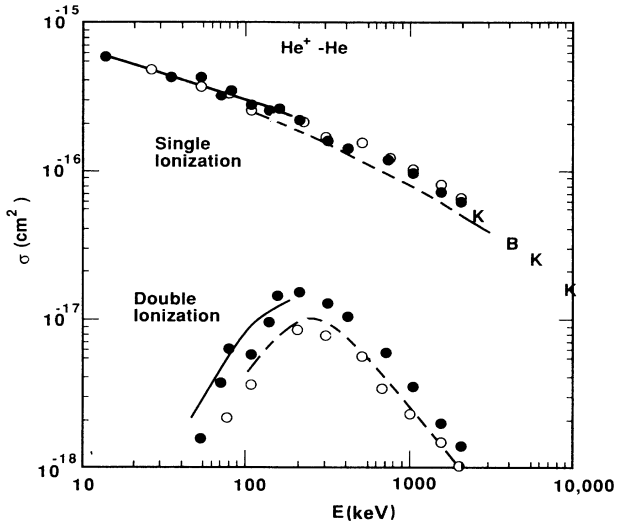

FIG. 3. Absolute cross sections for total single and total double ionization of helium by He^+. ●, present work; ○, data from Ref. 11 normalized to σ_+ cross sections of Ref. 1 as described in text; ——, Ref. 10; — — —, Ref. 13; *B*, Ref. 5; *K*, Ref. 20.

collisions,[19] presumably our earlier measurements suffered from a collection efficiency problem for ionized helium target ions.

Neon

Results for the ionization of neon are tabulated in Table II and shown in Fig. 4. Again the cross sections have been placed on an absolute scale by normalizing at each impact energy to the total slow positive-charge production cross sections σ_+ of Rudd *et al.*[1] The agreement between the remeasured cross sections (closed symbols) and the values obtained by normalizing to σ_+ (open symbols) is within combined experimental uncertainties with the latest results being approximately 20% larger except for triple ionization which is roughly 40% larger. Again, at the lowest impact energies, the present data yielding smaller total free-electron production cross sections σ_- than those reported by Rudd *et al.*[1] is confirmed. At higher energies, the agreement is excellent.

For neon, multiple ionization of the target is more important than for helium. For example, direct double ionization is approximately a factor of 5–10 less likely than is single ionization; a similar reduction occurs when going from direct double to triple ionization. In the case of of electron capture, the relative importance of the capture-plus-ionization channels tends to increase with impact energy. The electron-loss data show that the total electron-loss cross sections[1,2,6] are larger than the sum of the σ_q^{12} cross sections by an amount that is again attributed to pure electron loss σ_0^{12}. Again this cross section was deduced by subtracting $\sum_q \sigma_q^{12}$ from σ^{12}, where, as before, the σ^{12} cross sections reported in Refs. 1 and 2 were used. The deduced σ_0^{12} values (dotted curve) indicate that, for higher impact energies, ionization of the projectile generally results in ionization of the target as well. For example, $\sigma_1^{12} > \sigma_0^{12}$.

The overall accuracy of the present data can be determined by comparing to various total or partial cross sections that have previously been measured. For example,

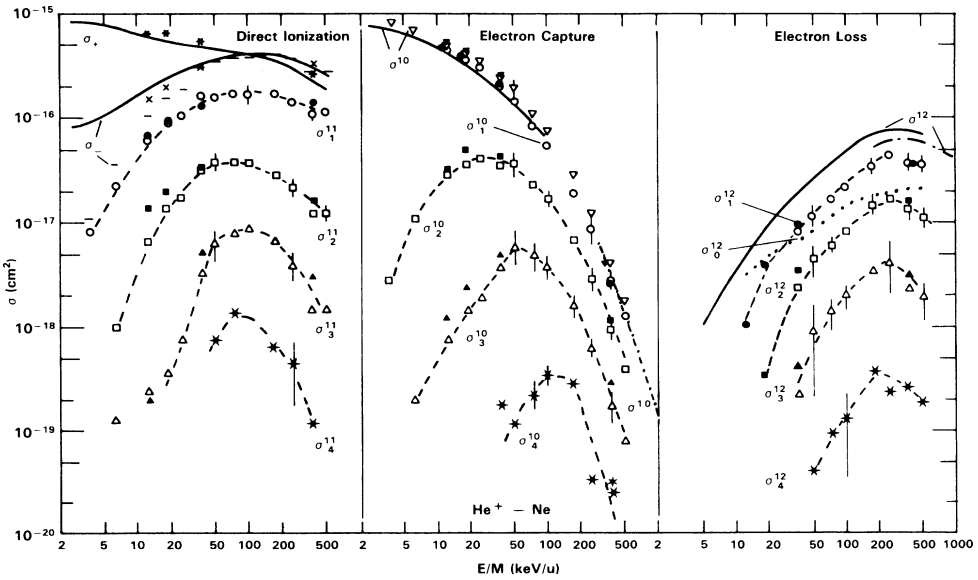

FIG. 4. Absolute cross sections for multiple ionization of neon by He^+ impact. Notation and data sources are the same as in Fig. 1 with the following exceptions. σ^{10}: ——, total single-electron capture cross sections from Refs. 1 and 2; —·—·—·, from Ref. 6; ▽, present work. σ_q^{1j}: cross sections for single to quadrupole ionization of neon, $q = 1$–4, ○, □, △, ∗, respectively. The superscripts represent the projectile initial and final charge states. The solid symbols, ∗, and × indicate remeasured cross sections as explained in the text.

TABLE II. Absolute cross sections (in units of 10^{-16} cm^2) for He^+-Ne collisions. The 3.75–25-keV/u cross sections are taken from Ref. 16 and have been reevaluated as described in the text. Otherwise the notation and uncertainties are as given in Table I.

				He^+-Ne												
				Direct ionization			Single-electron capture					Electron loss				
E/M keV/u	σ_+	σ_-	σ_1^{11}	σ_2^{11}	σ_3^{11}	σ_4^{11}	σ^{10}	σ_1^{10}	σ_2^{10}	σ_3^{10}	σ_4^{10}	σ_0^{12}	σ_1^{12}	σ_2^{12}	σ_3^{12}	σ_4^{12}
3.75	8.4	0.112	0.0834				8.28	8.25	0.0286							
6.25	7.4	0.366	0.229	0.009 84	0.001 22		7.03	6.92	0.112	0.0020						
12.5	5.9	1.07	0.616	0.0667	0.0024		4.84	4.54	0.294	0.0075						
18.8	5.5	1.59	0.912	0.139	0.0036		3.91	3.53	0.367	0.0146						
25	5.3	1.90	1.08	0.177	0.0074		3.40	2.97	0.410	0.0193						
37.5	4.9	3.13	1.66	0.311	0.0326		2.37	1.98	0.356	0.0367	0.001 82	0.078	0.0818	0.0227	0.002 18	
50	4.7	3.50	1.57	0.388	0.0631*	0.007 25	1.87	1.44	0.367*	0.0584*	0.001 21	0.074	0.116*	0.0453*	0.0089*	0.000 40
75	4.4	3.78	1.74	0.381	0.0799	0.0145	1.10	0.813	0.233	0.0497*	0.002 35*	0.117	0.167	0.0621*	0.0138*	0.000 94
100	4.2	3.90	1.71	0.379	0.0861		0.752	0.543	0.167	0.0388*	0.003 55	0.149	0.217	0.0830	0.0202*	0.001 30*
175	3.5	4.07	1.67	0.294	0.0665	0.006 50	0.283	0.196	0.0690	0.0162*	0.002 98	0.163	0.348	0.153	0.0340	0.003 79
250	3.0	3.72	1.43	0.223	0.0383*	0.004 56*	0.121*	0.0862*	0.0287*	0.006 23	0.000 33	0.112	0.434	0.168	0.0426*	0.002 28
375	2.3	2.87	1.08	0.125	0.0144	0.001 19	0.0412*	0.0296*	0.009 69*	0.001 79*	0.000 237	0.212	0.370*	0.134	0.0232	0.002 67
500	1.9	2.81	1.15	0.122	0.0144		0.0178	0.0129	0.004 09	0.000 78	0.000 83	0.208	0.368	0.114*	0.0190*	0.001 87

the present total capture cross sections are approximately 20% larger than those previously reported.[1,2,6] Other comparisons, not shown, demonstrate that the present relative target charge state fractions resulting from electron capture f_q^{10} are in good agreement with measurements by Schuch.[15] The total single ionization cross sections generated from the present data agree well with the measurements of Fedorenko and Afrosimov[10] and with cross sections determined from our earlier charge state fraction measurements[11] but for double and triple ionization, the present and earlier data obtained in our laboratory[11] agree within experimental uncertainties while the measurements of Fedorenko and Afrosimov[10] indicate larger cross sections for impact energies less than 100 keV.

The present data, when used to investigate the relative importance of the direct-ionization, electron-capture, and electron-loss channels toward the production of free electrons, indicate that the electron-capture-plus-ionization channels are responsible for about 25–30 % of the electron production for impact energies below 20 keV/u. Above 300 keV/u, the direct-ionization and the electron-loss channels each contribute roughly 50% to the free-electron production. Thus, the electron capture or loss channels are responsible for 25–50 % of the free-electron production throughout the entire energy range investigated with direct ionization being responsible for the remainder.

Measurements of subshell[21,22] and inner-shell[23] cross sections indicate that the single- and double-ionization cross sections shown in Fig. 4 are predominantly due to ionization of the $2p$ shell of neon. Thus neon $2p$ ionization is the dominant contributor to the ejected electron spectra resulting from He^+-Ne collisions with some contribution at higher impact energies due to ionization of the projectile.

Argon

Cross sections for ionization of argon are tabulated in Table III and shown graphically in Fig. 5. For argon, the renormalized and corrected cross sections presented here for energies less than 100 keV are approximately 10% larger than those given in Ref. 16 except for the lowest two energies where they are 30–40 % larger. Again, as was shown for helium and neon targets, the present values for σ_- are in good agreement with the measurements of Rudd *et al.*[1] above 100 keV but are consistently smaller for lower impact energies. This discrepancy is confirmed by our remeasured cross sections (closed symbols in Fig. 5). For argon, direct multiple ionization is more important than was found for helium and neon targets. Contributions from inner-shell ionization contributing to three-, four-, and five-times-ionized argon are indicated by the change in slope occurring for higher impact energies. These effects are evident in the ionization as well as the electron-capture and -loss channels and are consistent with the L-Auger spectral analysis done by Stolterfoht *et al.*[24]

As before, the present electron-capture data yield consistently larger (roughly 30% larger) total capture cross

TABLE III. Absolute cross sections (in units of 10^{-16} cm^2) for He^+-Ar collisions. Notation and uncertainties are as given for Table I.

			He^+-Ar															
			Direct ionization					Single-electron capture				Electron loss						
E/M keV/u	σ_+	σ_-	σ_1^{11}	σ_2^{11}	σ_3^{11}	σ_4^{11}	σ_5^{11}	σ^{10}	σ_1^{10}	σ_2^{10}	σ_3^{10}	σ_4^{10}	σ_1^{12}	σ_2^{12}	σ_3^{12}	σ_4^{12}	σ_5^{12}	
3.75	11.9	2.49	0.431	0.0466				9.41	7.50	1.88	0.0301							
6.25	13.1	3.71	0.671	0.166	0.0035			9.39	6.83	2.43	0.130							
12.5	14	5.36	1.26	0.456	0.0507			8.63	5.99	2.26	0.375							
18.8	13.9	6.73	1.85	0.759	0.141	0.0046		7.35	4.72	2.02	0.427	0.0204						
25	13.1	7.06	2.19	0.797	0.183	0.007 56		6.02	3.80	1.75	0.433	0.0266						
37.5	12.5	9.35	3.45	0.969	0.329*	0.0296*		5.18	3.33	1.41	0.411	0.0320	0.0841*	0.0622	0.0225*	0.0017		
50	12.0	9.98	4.08	1.05*	0.361*	0.0376*	0.004 83	3.32*	2.03*	1.01*	0.318*	0.0325*	0.176*	0.0933*	0.0337	0.003 02*	0.000 34	
75	10.5	10.4	4.32	1.04	0.307*	0.0292*	0.005 96	1.64*	0.998*	0.489	0.146*	0.008 43*	0.348*	0.192*	0.0720*	0.006 55*	0.001 18	
100	9.8	10.2	4.45	0.949	0.254*	0.0225*	0.006 07	0.706	0.500	0.230	0.0527	0.008 40*	0.528	0.335	0.106*	0.0118	0.002 53	
125	9.9	12.0	4.86	0.788	0.209	0.0139		0.525*	0.337*	0.143*	0.0382	0.0070*	0.878	0.561	0.166	0.0224		
175	8.0	9.70	4.00	0.570	0.107*	0.0182	0.005 51	0.190*	0.126*	0.541*	0.009 56*	0.000 66	0.969	0.514	0.120*	0.0157	0.003 94	
250	6.5	8.47	3.97	0.375	0.0611	0.008 20*	0.001 27	0.0603*	0.0444*	0.0140	0.004 17*	0.001 04	0.902	0.389	0.0955	0.0191*	0.006 97	
375	5.0	6.30	2.98	0.219	0.0382*	0.008 93*	0.005 71	0.0123	0.006 56	0.002 51	0.002 18	0.000 71	0.778	0.249	0.0664	0.0154*	0.004 67	
500	4.2	5.06	2.47	0.156	0.0260	0.0086*	0.006 01	0.003 37	0.000 56	0.001 76	0.000 90	0.000 15	0.630	0.175	0.0529*	0.0181	0.004 59	

sections than those previously reported.[1-3,6] For the electron-loss channels, within experimental uncertainties, the present data totally account for the total electron-loss cross section.[1,2,6] This implies that, in He^+-Ar collisions, ionization of the projectile *always* results in ionization of the target. The change in slope at higher impact energies indicate that triple and quadrupole ionization of argon occurring as a result of electron capture or loss is strongly influenced by inner-shell ionization.

Comparing the data presented here with previous measurements[10,11,15] indicate reasonably good agreement for single and double ionization but imply that the present measurements may underestimate the amount of higher degrees of ionization. Most likely these discrepancies result from target ion detection efficiency problems but could also result since the cross sections for higher degrees of target ionization decrease rapidly at low impact energies where the comparisons were made. To resolve these discrepancies additional measurements are required.

The relative importance of direct ionization, electron capture, and electron loss toward the production of free electrons is shown in Fig. 6. At low energies, the higher-order electron-capture channels are the primary source of electrons; in fact at the lowest energy shown, direct ionization is only responsible for 20% of the free-electron production. At high impact energies, the electron-loss and direct-ionization channels are of comparable magnitude. Information about the Auger channel[24] indicates that it makes a relatively unimportant contribution to either the double ionization or the total electron-production cross section.

Krypton

Results for krypton are given in Table IV and Fig. 7. Except for the increasing importance of the multiple ionization channels, the results are similar to those shown for the lighter targets. Again, at the lower impact energies, the present work yields smaller σ_- cross sections than those reported by Rudd *et al.*[1] and the present σ^{10} cross sections are 20–30 % larger than previous measurements[1,2] although the agreement improves at higher impact energies. In the electron-loss channel, the sum of the electron-loss cross sections indicates that there is little or no pure electron loss σ_0^{12}, except perhaps at the highest impact energies.

One interesting feature in the electron capture channels is that the σ_q^{10}, $q=2,3,4$, are larger than the "pure" electron-capture cross sections σ_1^{10} for impact energies greater than 300 keV/u. This was also observed for proton impact[19] and is due to the emergence of M-shell capture as the predominant capture channel. Capturing an M-shell electron leads to various Auger relaxation modes which increases the probability that the final target ionization states will be two or larger.

From these data, a determination of the relative importance of the various channels toward the total free-electron production cross section yields results similar to those shown in Fig. 6 for an argon target. Specifically, at low impact energies most of the free electrons are pro-

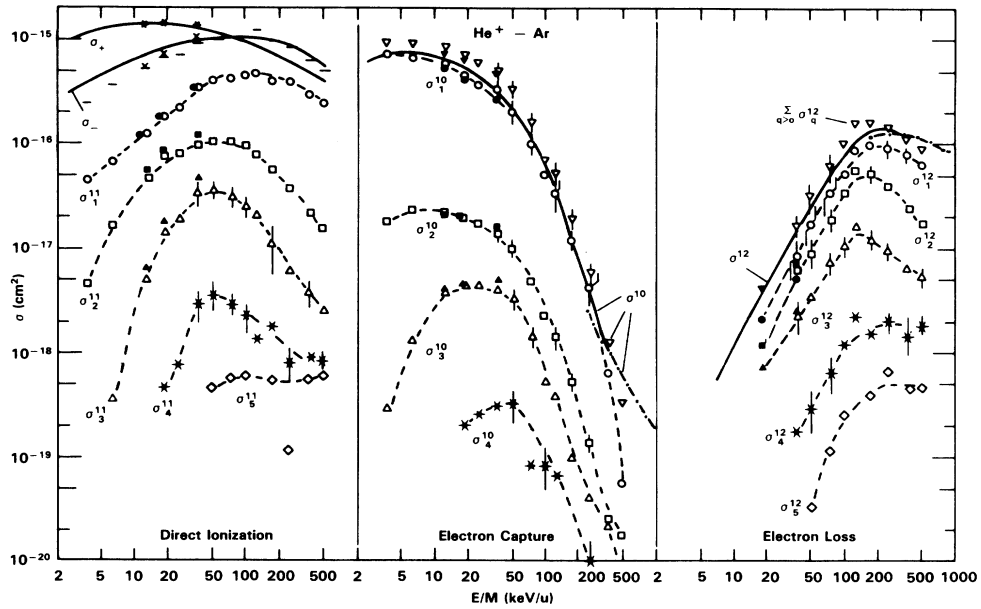

FIG. 5. Absolute cross sections for multiple ionization of argon by He^+ impact. Notation and data sources are the same as in Fig. 1 with the following exceptions. σ^{10}: ——, total single electron capture cross sections from Refs. 1 and 2; —·—·—·, from Ref. 6; ▽, present work. σ^{12}: ——, total single-electron loss cross sections from Refs. 1 and 2; —·—·—·, from Ref. 6. σ_q^{1j}: cross sections for single to five times ionized argon, $q = 1-5$, ○, □, △, *, ◇, respectively. $\sum_q \sigma_q^{12}$: ▽, total cross section for ionization of the projectile where the target is also ionized.

duced in electron capturing collisions; the direct-ionization channels are responsible for less than 20% of the free-electron production below 5 keV/amu. At the highest impact energy reported here, electron production from the direct-ionization and the electron-loss channels is equally probable. The importance of the direct-ionization channels toward the total electron-production cross section maximizes at 85% near 100 keV/amu.

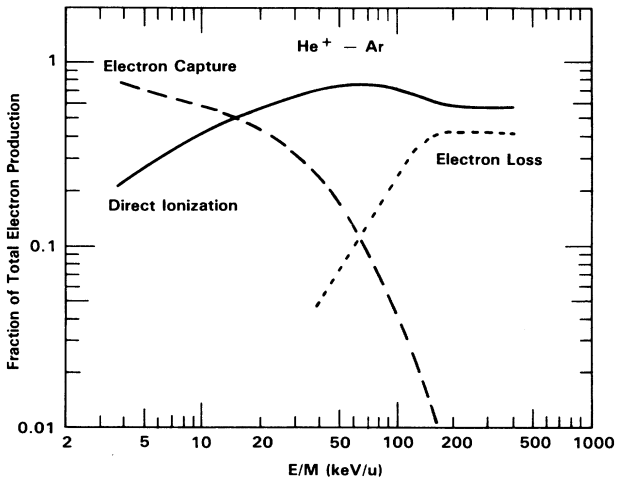

FIG. 6. Fraction of free-electron production due to direct-ionization electron-capture, and electron-loss channels in He^+-Ar collisions.

Comparing the present krypton charge state fractions with those previously reported[10,11,15] yields results similar to those found for argon—namely, the present single- and double-ionization results are in approximate (roughly 15%) agreement while for higher degrees of ionization the present results are considerably smaller than were measured in previous experiments. This is again attributed to target-ion detection efficiencies but it should be noted that to force agreement between the present cross sections and those reported by Fedorenko and Afrosimov,[10] a constant detection efficiency for charge states 1–3 and a monotonically decreasing detection efficiency for higher charge states would be required. This is in conflict with efficiency measurements performed for the present work. Hence, to resolve this question will require additional experimental investigations.

SUMMARY

Cross sections for single and multiple ionization resulting from direct ionization, electron capture, and electron loss have been presented for He^+ impact on rare-gas targets. When combined with various total cross sections, a detailed picture of ionization occurring in these collisions is obtained. The present data, which were placed on an absolute scale by normalizing to the total slow positive-charge-production cross sections σ_+ of Rudd *et al.* typically yield 20–30% larger total capture cross sections σ^{10} than have been previously reported. Thus the relative uncertainties in the cross sections for the various channels resulting from the data acquisition and normali-

TABLE IV. Absolute cross sections (in units of 10^{-16} cm^2) for He^+-Kr collisions. Notation and uncertainties are as given for Table I.

											He^+-Kr																
											Single-electron capture										Electron loss						
			Direct ionization																								
E/M																											
keV/u	σ_+	σ_-	σ_1^{11}	σ_2^{11}	σ_3^{11}	σ_4^{11}	σ_5^{11}	σ_6^{11}	σ_7^{11}	σ^{10}	σ_1^{10}	σ_2^{10}	σ_3^{10}	σ_4^{10}	σ_5^{10}	σ_6^{10}	σ_1^{12}	σ_2^{12}	σ_3^{12}	σ_4^{12}	σ_5^{12}	σ_6^{12}	σ_7^{12}
3.75	13.9	3.39	0.513	0.0475						10.5	7.75	2.74	0.0227										
6.25	15.5	4.81	0.670	0.145	0.00143					10.7	7.12	3.41	0.215										
12.5	17	6.79	1.63	0.391	0.0416	0.0080				10.2	6.56	3.09	0.540	0.0171									
18.8	16.8	8.07	2.35	0.614	0.119	0.0133				8.76	5.37	2.78	0.572	0.0529									
25	16.3	8.98	2.97	0.737	0.177	0.0231				7.29	4.19	2.36	0.661	0.0757									
37.5	15	8.52	3.42	0.686	0.207	0.0187				5.36	3.07	1.67	0.529	0.0781	0.0151	0.0023							
50	14.5	10.0	5.02	0.931	0.280	0.0404	0.0104	0.0033		2.90	1.41	1.00	0.407	0.0614	0.0134	0.0052							
75	14	12.6	6.25	1.29	0.375	0.0724	0.0391	0.0041		2.16	1.30	0.567	0.228	0.0476	0.0159	0.0059	0.199	0.0865	0.0368	0.0059	0.0038	0.0023	
100	13	12.2	6.14	1.24	0.341	0.0772	0.0344	0.0103		0.970	0.506	0.317	0.102	0.0350	0.0097		0.255	0.150	0.0703	0.0139	0.0065	0.0031	
175	11	11.7	5.85	0.778	0.206	0.0564	0.0348	0.0116	0.0021	0.197	0.110	0.0472	0.0237	0.0100	0.0041	0.0016	0.656	0.286	0.117	0.0464	0.0212	0.0079	0.0013
250	9.2	10.5	5.00	0.468	0.142	0.0401	0.0288	0.0097	0.0026	0.0595	0.0267	0.0139	0.0112	0.0041	0.00286	0.00055	0.785	0.308	0.132	0.0623	0.0341	0.0138	0.0043
375	7.8	9.15	4.03	0.297	0.108	0.0494	0.0264	0.0146	0.00509	0.0207	0.00268	0.00546	0.00622	0.00370	0.00169	0.00051	0.791	0.274	0.133	0.0666	0.0387	0.0178	0.00861
500	6.1	6.21	2.40	0.172	0.0754	0.0224	0.0190	0.00912	0.00282								0.645	0.191	0.120	0.0497	0.0377	0.0160	0.00522

zation processes are interpreted to be 20–30 %. The accuracy of the data and the normalization process were verified by using an independently calibrated system to repeat the measurements at a few selected energies.

The electron-loss data indicated that in He^+–rare-gas collisions, electron loss by the helium ion generally results in ionization of the target as well. This is because the collision must be sufficiently "hard" in order to strip the remaining 1*s* electron from He^+; but such hard collisions also tend to ionize the target. This "double-ionization" event where target ionization accompanies projectile ionization increases as the target-ionization potential decreases, e.g., it is largest for krypton and argon, smaller for neon, and smallest for helium targets. This mechanism was shown to be a significant contributor to the free-electron production at higher impact energies where detailed measurements of the electron emission spectra have been made for He^+-He collisions.[25] Forward emission of a "fast" electron having approximately the same velocity as the projectile ion and, in addition, isotropic emission of a low-energy electron was observed. The fast electron was attributed as coming from the projectile while the slower electron was attributed to target ionization accompanying the projectile ionization.

The present data also showed how the electron emission from heavier targets is dominated by the electron-capture-plus-ionization (σ_q^{10}, $q > 1$) channels for low impact energies, thus demonstrating how higher order channels can play a non-negligible role in free-electron production. Even for a helium target, the free-electron contribution from the σ_2^{10} channel is 10% of the total between 80 and 200 keV; for heavier targets the percentage is larger and sometimes dominant. Higher-order electron-loss channels play a significant role at higher impact energies where they can contribute up to half of the electrons liberated in the collision. Thus theoretical models of ionization occurring in He^+–rare-gas collisions need to include these multiple-ionization channels.

In comparing the present data with previously measured cross sections, it was observed that the present free-electron production cross sections σ_- agreed well with the measurements of Rudd *et al.* above 100 keV but gave increasingly smaller results for lower energy collisions. This had been observed previously[17] for He^{2+} impact on the same targets. Since the discrepancy occurred only for energies below 100 keV and these data had been obtained several years ago using an entirely different apparatus, the cross sections were remeasured for a few energies between 50 and 150 keV. Within experimental uncertainties, complete agreement was found with the original coincidence data. Thus a discrepancy exists between the total electron production cross sections obtained using the present method and those obtained using the condenser plate method.[1] An investigation into this discrepancy is currently in progress but some comments can be made at this time.

The present method has several advantages; namely, the beam purity with and without target gas present is precisely known, target ionization can be distinguished from background gas ionization, and since the target ions are detected, the present method is insensitive to the

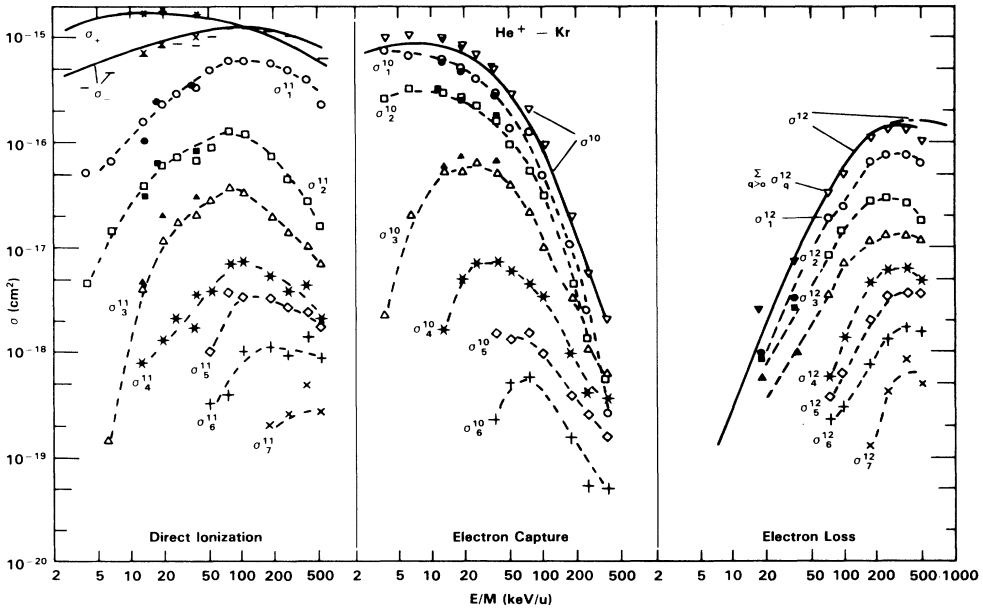

FIG. 7. Absolute cross sections for multiple ionization of krypton by He^+ impact. Notation and data sources are the same as in Fig. 1 with the following exceptions. σ^{10}: ——, total single-electron-capture cross sections from Refs. 1 and 2; ▽, present work. σ^{12}: ——, total single-electron-loss cross sections from Refs. 1 and 2; —·—·—·, from Ref. 6. $\sigma_q^{1,j}$: cross sections for single to seven times ionized krypton, $q=1$–7, ○, □, △, *, ◇, +, ×, respectively. $\sum_q \sigma_q^{12}$: ▽, total cross section for ionization of the projectile where the target is also ionized.

large number of stray electrons that can contribute to the σ_- signal in the condenser-plate method. An obvious disadvantage of the present method is that several quantities must be accurately measured and summed to determine σ_-. However, the present method was shown to yield accurate values for σ_- at higher impact energies. Another disadvantage is that the present method relies on measurements of beam detection efficiencies made at higher impact energies. If these efficiencies change for lower impact energies, the measured cross sections and hence the σ_- results will be affected. However, this would also effect the total capture cross sections which are shown to be in reasonable agreement with previously measured values. Another possibility, although not considered to be very likely because of the pressures used, is that a second collision could alter the post-collision projectile charge state after the target ionization has occurred and thus a target ionization event could appear in the capture channel or vice versa. However, no such affects could be observed when searched for. Thus, the present measurements of σ_- are considered to be accurate. A reexamination of the cross-section data reported in Ref. 1 is in progress to see if any errors or inconsistencies can be identified.

Total cross sections for single and multiple ionization σ_q^T determined from the present data were compared to those reported by Fedorenko and Afrosimov and to values determined from total charge state fractions that were previously measured in our laboratory. Generally all three sets of data demonstrated the same impact energy dependence although the relative percentages of single and multiple ionization differed in some cases. For example, compared to the data presented here, our previous measurements were shown to underestimate the amount of double ionization in helium, to be in good agreement for neon, but to slightly underestimate the amount of single ionization in argon and krypton while overestimating the amount of triple and quadruple ionization. These same conclusions were drawn from an analysis of available data leading to multiple ionization of He, Ne, Ar, and Kr by proton impact.[19] It is felt that the early data may be subject to recoil ion transmission and detection efficiency problems for the helium, argon and krypton targets although no specific errors can be identified. However, the data of Fedorenko and Afrosimov and the capture data of Schuch indicate that the present work underestimates the cross sections for higher charge states or the heavier targets but by a lesser amount than our previous data indicated. Clearly, additional work is required to resolve this problem for high degrees of ionization of argon and krypton targets and also to resolve the σ_- problem.

ACKNOWLEDGMENTS

Work supported by the Office of Health and Environmental Research (OHER), U.S. Department of Energy, under Contract No. DE-AC06-76RL0 1830.

[1]M. E. Rudd, T. V. Goffe, A. Itoh, and R. D. DuBois, Phys. Rev. A **32**, 829 (1985).

[2]Y. Nakai, A. Kikuchi, T. Shirai, and M. Sataka, Japan Atomic Energy Research Institute Report No. JAERI-M 84-069, 1984 (unpublished). This report tabulates cross sections for helium ions impacting on rare gases. Data specific to the systems and impact energies studied in the present work include measurements by C. F. Barnett and P. M. Stier, Phys. Rev. **109**, 385 (1958); F. J. deHeer, J. Schutten, and H. Moustafa, Physica **32**, 1973 (1966); N. V. Fedorenko, V. V. Afrosimov, and D. M. Kaminker, Zh. Tekh. Fiz. **26**, 1929 (1956) [Sov. Phys.—Tech. Phys. **1**, 1861 (1956)]; Ya. M. Fogel', V. A. Ankudinov, and D. V. Pilipenko, Zh. Eksp. Teor. Fiz. **38**, 26 (1960) [Sov. Phys.—JETP **11**, 18 (1960)]; H. B. Gilbody, K. F. Dunn, R. Browning, and C. J. Latimer, J. Phys. B **3**, 1105 (1970); **4**, 800 (1971); E. Horsdal Pedersen and P. Hvelplund, *ibid.* **7**, 132 (1974); E. Horsdal Pedersen, J. Heinemeier, J. Larsen, and J. Mikkelsen, *ibid.* **13**, 1167 (1980); P. Hvelplund and E. Horsdal Pedersen, Phys. Rev. A **9**, 2434 (1974); L. I. Pivovar, V. M. Tubaev, and M. T. Novikov, Zh. Eksp. Teor. Fiz. **41**, 26 (1961) [Sov. Phys.—JETP **14**, 20 (1962)].

[3]C. F. Barnett, J. A. Ray, E. Ricci, M. I. Wilker, E. W. McDaniel, E. W. Thomas, and H. B. Gilbody, Oak Ridge National Laboratory Report No. ORNL-5206, 1977, Vol. I (unpublished).

[4]H. K. Haugen, L. H. Andersen, P. Hvelplund, and H. Knudsen, Phys. Rev. A **26**, 1950 (1982).

[5]S. H. Be, T. Tonuma, H. Kumagai, H. Shibata, M. Kase, T. Kambara, I. Kohno, and H. Tawara, J. Phys. B **19**, 1771 (1986).

[6]N. V. de Castro Faria, F. L. Freire, Jr., and A. G. de Pinho, Phys. Rev. A **37**, 280 (1988).

[7]K. L. Bell, V. Dose, and A. E. Kingston, J. Phys. B **3**, 129 (1969).

[8]C. K. Tan and A. R. Lee, J. Phys. B **14**, 2409 (1981); **14**, 3445 (1981).

[9]T. Kaneko, Phys. Rev. A **32**, 2175 (1985); **34**, 1779 (1986).

[10]N. V. Fedorenko and V. V. Afrosimov, Zh. Tekh. Fiz. **26**, 1941 (1956) [Sov. Phys.—Tech. Phys. **1**, 1872 (1956)].

[11]R. D. DuBois, L. H. Toburen, and M. E. Rudd, Phys. Rev. A **29**, 70 (1984).

[12]A. K. Edwards, R. M. Wood, and R. L. Ezell, Phys. Rev. A **32**, 1346 (1985).

[13]R. M. Wood, A. E. Edwards, and R. L. Ezell, Phys. Rev. A **34**, 4415 (1986).

[14]P. Hvelplund, H. K. Haugen, and H. Knudsen, Phys. Rev. A **22**, 1930 (1980).

[15]B. Schuch, Diplomarbeit, Universität Giessen, 1984.

[16]R. D. DuBois, Phys. Rev. Lett. **52**, 2348 (1984).

[17]R. D. DuBois, Phys. Rev. A **36**, 2585 (1987).

[18]R. D. DuBois, Nucl. Instrum. Methods **B24/25**, 209 (1987).

[19]R. D. DuBois and S. T. Manson, Phys. Rev. A **35**, 2007 (1987).

[20]H. Knudsen, L. H. Andersen, P. Hvelplund, G. Astner, H. Cederquist, H. Danared, L. Liljeby, and K.-G. Rensfelt, J. Phys. B **17**, 3545 (1984).

[21]R. Hippler and K.-H. Schartner, Z. Phys. A **273**, 123 (1975).

[22]H. F. Beyer, R. Hippler, and K.-H. Schartner, Z. Phys. **292**, 353 (1979).

[23]N. Stolterfoht and D. Schneider, Phys. Rev. A **11**, 721 (1975).

[24]N. Stolterfoht, D. Schneider, and P. Ziem, Phys. Rev. A **10**, 81 (1974).

[25]R. D. DuBois and S. T. Manson, Phys. Rev. Lett. **57**, 1130 (1986).